

1 Inferring the effective start dates of non-pharmaceutical  
2 interventions during COVID-19 outbreaks

3 Ilia Kohanovski<sup>a</sup>, Uri Obolski<sup>b,c</sup>, and Yoav Ram<sup>a,\*</sup>

4 <sup>a</sup>School of Computer Science, Interdisciplinary Center Herzliya, Herzliya 4610101, Israel

5 <sup>b</sup>School of Public Health, Tel Aviv University, Tel Aviv 6997801, Israel

6 <sup>c</sup>Porter School of the Environment and Earth Sciences, Tel Aviv University, Tel Aviv 6997801, Israel

7 \*Corresponding author: yoav@yoavram.com

8 May 20, 2020

9 **Abstract**

10 During February and March 2020, several countries implemented non-pharmaceutical inter-  
11 ventions, such as school closures and lockdowns, with variable schedules to control the COVID-19  
12 pandemic caused by the SARA-CoV-2 virus. Overall, these interventions seem to have success-  
13 fully reduced the spread of the pandemic. We hypothesize that the official and effective start  
14 date of such interventions can significantly differ, for example due to slow diffusion of guidelines  
15 in the population, or due to unpreparedness of the authorities and the public. We use an SEIR  
16 epidemiological model and an MCMC inference framework to estimate the effective start of NPIs  
17 in several countries, and compare this effective dates to the official dates. We report our finding of  
18 both late and early effects of NPIs, and discuss potential causes and consequences of our results.

## 19 Introduction

20 The COVID-19 pandemic has resulted in implementation of extreme non-pharmaceutical interventions  
21 (NPIs) in many affected countries. These interventions, from social distancing to lockdowns, are  
22 applied in a rapid and widespread fashion. The NPIs are designed and assessed using epidemiological  
23 models, which follow the dynamics of the viral infection to forecast the effect of different mitigation and  
24 suppression strategies on the levels of infection, hospitalization, and fatality. These epidemiological  
25 models usually assume that the effect of NPIs on disease transmission begins at the officially declared  
26 date (e.g. Flaxman et al.<sup>6</sup>, Gatto et al.<sup>8</sup>, Li et al.<sup>12</sup>).

27 Adoption of public health recommendations is often critical for effective response to infectious dis-  
28 eases, and has been studied in the context of HIV<sup>11</sup> and vaccination<sup>4,17</sup>, for example. However,  
29 behavioral and social change does not occur immediately, but rather requires time to diffuse in the  
30 population through media, social networks, and social interactions. Moreover, compliance to NPIs  
31 may differ between different interventions and between people. For example, in a survey of 2,108  
32 adults in the UK during Mar 2020, Atchison et al.<sup>2</sup> found that those over 70 years old were more  
33 likely to adopt social distancing than young adults (18-34 years old), and that those with lower income  
34 were less likely to be able to work from home and to self-isolate. Similarly, compliance to NPIs may  
35 be impacted by personal experiences. Smith et al.<sup>14</sup> have surveyed 6,149 UK adults in late April  
36 and found that people who believe they have already had COVID-19 are more likely to think they are  
37 immune, and less likely to comply with social distancing measures. Compliance may also depend on  
38 risk perception as perceived by the the number of domestic cases or even by reported cases in other  
39 regions and countries. Interestingly, the perceived risk of COVID-19 infection has likely caused a  
40 reduction in the number of influenza-like illness cases in the US starting from mid-February<sup>18</sup>.

41 Here, we hypothesize that there is a significant difference between the official start of NPIs and their  
42 adoption by the public and therefore their effect on transmission dynamics. We use a *Susceptible-*  
43 *Exposed-Infected-Recovered* (SEIR) epidemiological model and *Markov Chain Monte Carlo* (MCMC)  
44 parameter estimation framework to estimate the effective start date of NPIs from publicly available  
45 COVID-19 case data in several geographical regions. We compare these estimates to the official dates  
46 and find both late and early effects of NPIs on COVID-19 transmission dynamics. We conclude by  
47 demonstrating how differences between the official and effective start of NPIs can confuse assessments  
48 of the effectiveness of the NPIs in a simple epidemic control framework.

## 49 Models and Methods

50 **Data.** We use daily confirmed case data  $\mathbf{X} = (X_1, \dots, X_T)$  from several different countries. These  
51 incidence data summarize the number of individuals  $X_t$  tested positive for SARS-CoV-2 RNA (using  
52 RT-qPCR) at each day  $t$ . Data for Wuhan, China retrieved from Pei and Shaman<sup>13</sup>, data for 11  
53 European countries retrieved from Flaxman et al.<sup>6</sup>. Regions in which there were multiple sequences  
54 of days with zero confirmed cases (e.g. France), we cropped the data to begin with the last sequence  
55 so that our analysis focuses on the first sustained outbreak rather than isolated imported cases. For  
56 dates of official NPI dates see Table S1.

57 **SEIR model.** We model SARS-CoV-2 infection dynamics by following the number of susceptible  
58  $S$ , exposed  $E$ , reported infected  $I_r$ , and unreported infected  $I_u$  individuals in a population of size  $N$ .  
59 This model distinguishes between reported and unreported infected individuals: the reported infected  
60 are those that have enough symptoms to eventually be tested and thus appear in daily case reports, to  
61 which we fit the model.

Country	First	Last
Austria	Mar 10 2020	Mar 16 2020
Belgium	Mar 12 2020	Mar 18 2020
Denmark	Mar 12 2020	Mar 18 2020
France	Mar 13 2020	Mar 17 2020
Germany	Mar 12 2020	Mar 22 2020
Italy	Mar 5 2020	Mar 11 2020
Norway	Mar 12 2020	Mar 24 2020
Spain	Mar 9 2020	Mar 14 2020
Sweden	Mar 12 2020	Mar 18 2020
Switzerland	Mar 13 2020	Mar 20 2020
United Kingdom	Mar 16 2020	Mar 24 2020
Wuhan	Jan 23 2020	Jan 23 2020

**Table 1: Official start of non-pharmaceutical interventions.** The date of the first intervention is for a ban of public events, or encouragement of social distancing, or for school closures. In all countries except Sweden, the date of the last intervention is for a lockdown. In Sweden, where a lockdown was not ordered during the studied dates, the last date is for school closures. Dates for European countries from Flaxman et al.<sup>6</sup>, date for Wuhan, China from Pei and Shaman<sup>13</sup>. See Figure S1 for a visual presentation.

62 Susceptible ( $S$ ) individuals become exposed due to contact with reported or unreported infected  
 63 individuals ( $I_r$  or  $I_u$ ) at a rate  $\beta_t$  or  $\mu\beta_t$ . The parameter  $0 < \mu < 1$  represents the decreased transmission  
 64 rate from unreported infected individuals, who are often subclinical or even asymptomatic. The  
 65 transmission rate  $\beta_t \geq 0$  may change over time  $t$  due to behavioral changes of both susceptible and  
 66 infected individuals. Exposed individuals, after an average incubation period of  $Z$  days, become  
 67 reported infected with probability  $\alpha_t$  or unreported infected with probability  $(1 - \alpha_t)$ . The reporting  
 68 rate  $0 < \alpha_t < 1$  may also change over time due to changes in human behavior. Infected individuals  
 69 remain infectious for an average period of  $D$  days, after which they either recover, or becomes ill  
 70 enough to be quarantined. They therefore no longer infect other individuals, and the model does not  
 71 track their frequency. The model is described by the following equations:

$$\begin{aligned}
 \frac{dS}{dt} &= -\beta_t S \frac{I_r}{N} - \mu\beta_t S \frac{I_u}{N} \\
 \frac{dE}{dt} &= \beta_t S \frac{I_r}{N} + \mu\beta_t S \frac{I_u}{N} - \frac{E}{Z} \\
 \frac{dI_r}{dt} &= \alpha_t \frac{E}{Z} - \frac{I_r}{D} \\
 \frac{dI_u}{dt} &= (1 - \alpha_t) \frac{E}{Z} - \frac{I_r}{D}.
 \end{aligned} \tag{1}$$

72  
 73 The initial numbers of exposed  $E(0)$  and unreported infected  $I_u(0)$  are considered model parameters,  
 74 whereas the initial number of reported infected is assumed to be zero  $I_r(0) = 0$ , and the number of  
 75 susceptible is  $S(0) = N - E(0) - I_u(0)$ . This model is inspired by Li et al.<sup>12</sup> and Pei and Shaman<sup>13</sup>,  
 76 who used a similar model with multiple regions and constant transmission  $\beta$  and reporting rate  $\alpha$  to  
 77 infer COVID-19 dynamics in China and the continental US, respectively.

78 **Likelihood function.** For a given vector  $\theta$  of model parameters the *expected* cumulative number of  
 79 reported infected individuals ( $I_r$ ) until day  $t$  is, following Eq. (1),

$$Y_t(\theta) = \int_0^t \alpha_s \frac{E(s)}{Z} ds, \quad Y_0 = 0. \tag{2}$$

81 We assume that reported infected individuals are confirmed and therefore observed in the daily case  
 82 report of day  $t$  with probability  $p_t$  (note that an individual can only be observed once, and that  $p_t$   
 83 may change over time, but  $t$  is a specific date rather than the time elapsed since the individual was  
 84 infected). We denote by  $X_t$  the number of confirmed cases in day  $t$ , and by  $\tilde{X}_t$  the cumulative number  
 85 of confirmed cases until day  $t$ ,

$$86 \quad \tilde{X}_t = \sum_{i=1}^t X_i. \quad (3)$$

87 Therefore, at day  $t$  the number of reported infected yet-to-be confirmed individuals is  $(Y_t(\theta) - \tilde{X}_{t-1})$ .  
 88 We therefore assume that  $X_t$  conditioned on  $\tilde{X}_{t-1}$  is Poisson distributed,

$$89 \quad \begin{aligned} (X_1 | \theta) &\sim Poi(Y_1(\theta) \cdot p_1), \\ (X_t | \tilde{X}_{t-1}, \theta) &\sim Poi((Y_t(\theta) - \tilde{X}_{t-1}) \cdot p_t), \quad t > 1. \end{aligned} \quad (4)$$

90 Hence, the *likelihood function*  $\mathbb{L}(\theta | \mathbf{X})$  for the parameter vector  $\theta$  given the confirmed case data  
 91  $\mathbf{X} = (X_1, \dots, X_T)$  is defined by the probability to observe  $\mathbf{X}$  given  $\theta$ ,

$$92 \quad \mathbb{L}(\theta | \mathbf{X}) = P(\mathbf{X} | \theta) = P(X_1 | \theta) \cdot P(X_2 | \tilde{X}_1, \theta) \cdots P(X_T | \tilde{X}_{T-1}, \theta). \quad (5)$$

93 **NPI model.** To model non-pharmaceutical interventions (NPIs), we set the beginning of the NPIs  
 94 to day  $\tau$  and define

$$95 \quad \beta_t = \begin{cases} \beta, & t < \tau \\ \beta\lambda, & t \geq \tau \end{cases}, \quad \alpha_t = \begin{cases} \alpha_1, & t < \tau \\ \alpha_2, & t \geq \tau \end{cases}, \quad p_t = \begin{cases} 1/9, & t < \tau \\ 1/6, & t \geq \tau \end{cases}, \quad (6)$$

96 where  $0 < \lambda < 1$ . The values for  $p_t$  follow Li et al.<sup>12</sup>, who estimated the average time between  
 97 infection and reporting in Wuhan, China, at 9 days before the start of NPIs and 6 days after start of  
 98 NPIs.

99 **Parameter estimation.** To estimate the model parameters from the daily case data  $\mathbf{X}$ , we apply a  
 100 Bayesian inference approach. We start our model  $\Delta t$  days<sup>8</sup> before the outbreak (defined as consecutive  
 101 days with increasing confirmed cases) in each country. The model in Eq. (1) is parameterized by the  
 102 vector  $\theta$ , where

$$103 \quad \theta = (Z, D, \mu, \{\beta_t\}, \{\alpha_t\}, \{p_t\}, E(0), I_u(0), \tau, \Delta t). \quad (7)$$

104 The likelihood function is defined in Eq. (5). The posterior distribution of the model parameters  
 105  $P(\theta | \mathbf{X})$  is estimated using an *affine-invariant ensemble sampler for Markov chain Monte Carlo*  
 106 (MCMC)<sup>10</sup> implemented in the emcee Python package<sup>7</sup>.

107 We defined the following prior distributions on the model parameters  $P(\theta)$ :

$$\begin{aligned} Z &\sim \text{Uniform}(2, 5) \\ D &\sim \text{Uniform}(2, 5) \\ \mu &\sim \text{Uniform}(0.2, 1) \\ \beta &\sim \text{Uniform}(0.8, 1.5) \\ \lambda &\sim \text{Uniform}(0, 1) \\ \alpha_1, \alpha_2 &\sim \text{Uniform}(0.02, 1) \\ E(0) &\sim \text{Uniform}(0, 3000) \\ I_u(0) &\sim \text{Uniform}(0, 3000) \\ \Delta t &\sim \text{Uniform}(1, 5) \\ \tau &\sim \text{TruncatedNormal}\left(\frac{\tau^* + \tau^0}{2}, \frac{\tau^* - \tau^0}{2}, 1, T - 2\right), \end{aligned} \tag{8}$$

109 where the prior for  $\tau$  is a truncated normal distribution shaped so that the date of the first and last NPI,  
110  $\tau^0$  and  $\tau^*$  (Table S1), are at minus and plus one standard deviation, and taking values only between  
111 1 and  $T - 2$ , where  $T$  is the number of days in the data  $\mathbf{X}$ . We have also tested an uninformative  
112 uniform prior  $U(1, T - 2)$ . The uninformative prior could result in non-negligible posterior probability  
113 for unreasonable  $\tau$  values, such as Mar 1 in the United Kingdom. This was probably due to MCMC  
114 chains being stuck in low posterior regions of the parameter space. We therefore decided to use the  
115 more informative truncated normal prior. Other priors follow Li et al.<sup>12</sup>, with the following exceptions.  
116  $\lambda$  is used to ensure transmission rates are lower after the start of the NPIs ( $\lambda < 1$ ). We checked values  
117 of  $\Delta t$  larger than five days and found they generally produce lower likelihood, higher DIC (see below),  
118 and unreasonable parameter estimates, and therefore chose  $U(1, 5)$  as the prior.

119 **Model selection.** We perform model selection using DIC (deviance information criterion)<sup>15</sup>,

$$\begin{aligned} 120 \quad DIC(\theta, \mathbf{X}) &= 2\mathbb{E}[D(\theta)] - D(\mathbb{E}[\theta]) \\ &= 2\log \mathcal{L}(\mathbb{E}[\theta] \mid \mathbf{X}) - 4\mathbb{E}[\log \mathcal{L}(\theta \mid \mathbf{X})], \end{aligned} \tag{9}$$

121 where  $D(\theta) = -2\log \mathcal{L}(\theta \mid \mathbf{X})$  is the Bayesian deviance, and expectations  $\mathbb{E}[\cdot]$  are taken over the pos-  
122 terior distribution  $P(\theta \mid \mathbf{X})$ . We compare models by reporting their relative DIC; lower is better.

123 **Source code.** We use Python 3 with the NumPy, Matplotlib, SciPy, Pandas, Seaborn, and emcee  
124 packages. All source code will be publicly available under a permissive open-source license at  
125 [github.com/yoavram-lab/EffectiveNPI](https://github.com/yoavram-lab/EffectiveNPI). Files containing samples from the posterior distributions will  
126 be deposited on FigShare.

## 127 Results

128 Several studies have described the effects of non-pharmaceutical interventions in different geographical  
129 regions<sup>6,8,12</sup>. These studies have assumed that the parameters of the epidemiological model change  
130 at a specific date, as in Eq. (6), and set the change date  $\tau$  to the official NPI date  $\tau^*$  (Table S1). They  
131 then fit the model once for time  $t < \tau^*$  and once for time  $t \geq \tau^*$ . For example, Li et al.<sup>12</sup> estimate  
132 the dynamics in China before and after  $\tau^*$  at Jan 23. Thereby, they effectively estimate  $(\beta, \alpha_1)$  and  
133  $(\lambda, \alpha_2)$  separately. Here we estimate the posterior distribution  $P(\tau \mid \mathbf{X})$  of the *effective* start date of the  
134 NPIs by jointly estimating  $\tau, \beta, \lambda, \alpha_1, \alpha_2$  on the entire data per region (e.g. Italy, Austria), rather than

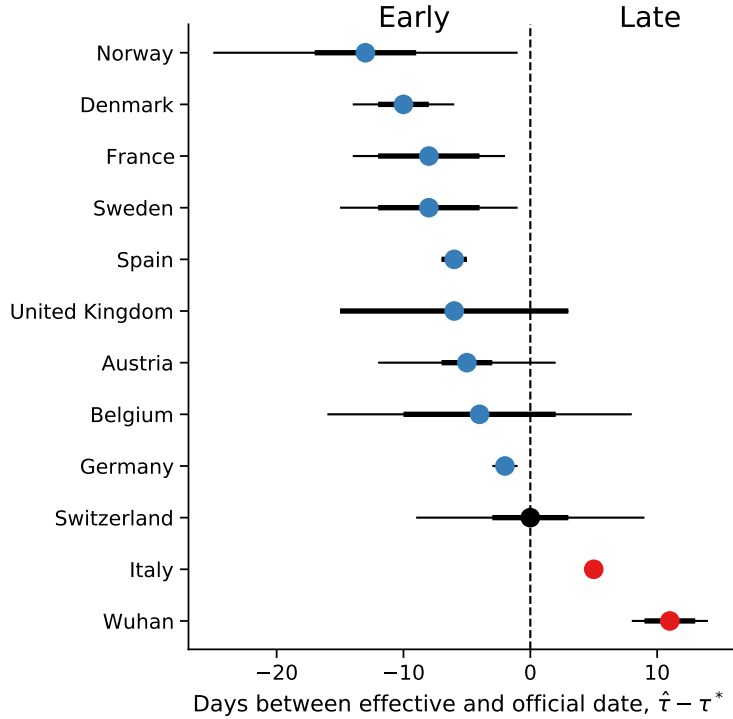


**Figure 1: Official and effective start of non-pharmaceutical interventions.** The difference between  $\hat{\tau}$  the effective and  $\tau^*$  the official start of NPI is shown for different regions. The effective NPI dates in Italy and Wuhan are significantly delayed compared to the official dates, whereas in Denmark, France, Spain, and Germany, the effective date is earlier than the official date.  $\hat{\tau}$  is the posterior median, see Table 2.  $\tau^*$  is the last NPI date, see Table S1. Thin and bold lines show 95% and 75% credible intervals (area in which  $P(|\tau - \hat{\tau}| \mid \mathbf{X}) = 0.95$  and 0.75.)

135 splitting the data at  $\tau^*$ . We then estimate the posterior probability  $P(\tau \mid \mathbf{X})$  by marginalizing the joint  
 136 posterior, and estimate  $\hat{\tau}$  as the posterior median.

137 We compared the **posterior predictive plots** of a model with a free  $\tau$  with those of a model with  $\tau$  fixed  
 138 at  $\tau^*$  and without  $\tau$ . The model with free  $\tau$  clearly produces better and less variable predictions (Fig-  
 139 ure S2a). **A similar comparison to no  $\tau$ .** However, when we compared the models using WAIC (??),  
 140 the model with a free parameter for the start of the NPI was better than the other models only in half  
 141 of the regions.

142 We compare the official  $\tau^*$  and effective  $\hat{\tau}$  start of NPIs and find that in most regions the effective start  
 143 of NPI significantly differs from the official date (Figure 1). Indeed, the credible interval on  $\hat{\tau}$  does  
 144 not include  $\tau^*$  (Figure 1). In the following, we describe our findings on late and early effective start of  
 145 NPI in detail.

Country	$\tau^*$	$\tau$	75% CI	95% CI	DIC using	Z	D	$\mu$	$\beta$	$\alpha_1$	$\lambda$	$\alpha_2$	E(0)	$I_u(0)$	$\Delta t$
Austria	Mar 16	Mar 11	2.0	7.0	29.62	3.92	3.59	0.43	1.10	0.06	0.73	0.45	464.24	555.98	2.0
Belgium	Mar 18	Mar 14	6.0	12.0	1.61	3.95	3.56	0.43	1.09	0.22	0.84	0.43	364.73	464.54	2.0
Denmark	Mar 18	Mar 08	2.0	4.0	10.23	3.96	3.47	0.37	1.06	0.04	0.32	0.53	501.86	638.74	2.0
France	Mar 17	Mar 09	4.0	6.0	-456.41	4.00	3.70	0.56	1.14	0.20	0.66	0.45	530.90	607.66	1.0
Germany	Mar 22	Mar 20	0.0	1.0	154.74	3.77	4.05	0.75	1.21	0.30	0.80	0.12	178.64	112.04	2.0
Italy	Mar 11	Mar 16	0.0	0.0	-6094.77	4.16	2.79	0.50	1.00	0.53	0.46	0.53	935.34	1928.88	1.0
Norway	Mar 24	Mar 11	4.0	12.0	-151.02	4.04	3.46	0.41	1.07	0.13	0.68	0.27	353.40	486.72	2.0
Spain	Mar 14	Mar 08	1.0	1.0	-55.73	3.94	3.62	0.61	1.11	0.07	0.73	0.53	898.03	897.61	2.0
Sweden	Mar 18	Mar 10	4.0	7.0	-258.97	4.02	3.50	0.42	1.06	0.11	0.64	0.25	386.21	494.37	2.0
Switzerland	Mar 20	Mar 20	3.0	9.0	-105.13	3.95	3.74	0.62	1.11	0.18	0.47	0.21	203.22	230.43	2.0
United Kingdom	Mar 24	Mar 18	9.0	9.0	12.13	3.98	3.82	0.54	1.15	0.21	0.83	0.39	268.76	260.68	2.0
Wuhan, China	Jan 23	Feb 03	2.0	3.0	27.03	3.73	3.63	0.61	1.15	0.28	0.18	0.35	597.87	561.16	2.0

**Table 2: Parameter estimates for different regions.** See Eq. (1) for model parameters. All estimates are posterior medians. 75% and 95% credible intervals given only for  $\tau$ , in days.  $\tau^*$  is the official last NPI date, see Table S1.

146 **Late effective start of NPIs.** In both Wuhan, China, and in Italy we find that our estimated effective  
 147 start of NPI  $\hat{\tau}$  is significantly later than the official date  $\tau^*$  (Figure 1).

148 In Italy, the first case was officially confirmed on Feb 21. School closures were implemented on  
 149 Mar 5<sup>6</sup>, a lockdown was declared in Northern Italy on Mar 8, with social distancing implemented  
 150 in the rest of the country, and the lockdown was extended to the entire nation on Mar 11<sup>8</sup>. That is,  
 151 the first and last official dates are Mar 8 and Mar 11. However, we estimate the effective date  $\hat{\tau}$  at  
 152 Mar 16 ( $\pm 0.47$  days 95% CI ; Figure 2). Similarly, in Wuhan, China, a lockdown was ordered on Jan  
 153 23<sup>12</sup>, but we estimate the effective start of NPIs to be several days later at Feb 2 ( $\pm 2.85$  days 95% CI  
 154 Figure 2).

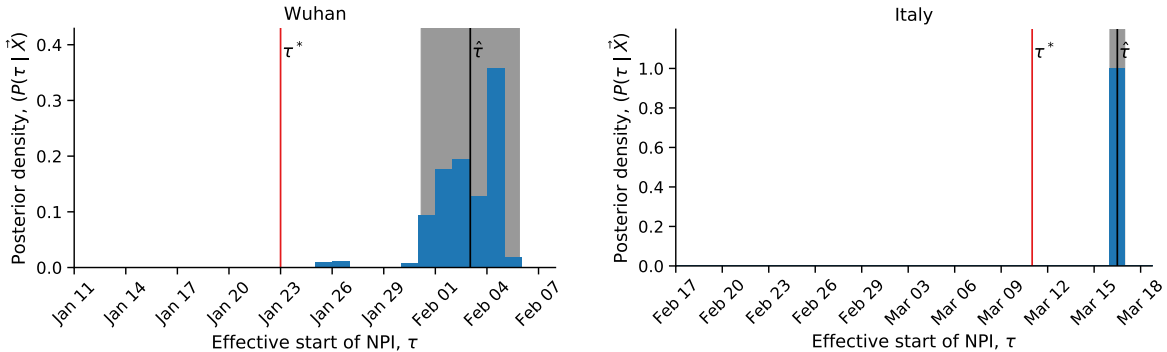


**Figure 2: Late effect of non-pharmaceutical interventions in Italy and Wuhan, China.** Posterior distribution of  $\tau$ , the effective start date of NPI, is shown as a histogram of MCMC samples. Red line shows the official last NPI date  $\tau^*$ . Black line shows the estimated  $\hat{\tau}$ . Shaded area shows a 95% credible interval (area in which  $P(|\tau - \hat{\tau}| \mid \mathbf{X}) = 0.95$ ).

155 **Early effective start of NPIs.** In contrast, in some regions we estimate an effective start of NPIs  $\hat{\tau}$   
 156 that is *earlier* than the official date  $\tau^*$  (Figure 1). In Spain, social distancing was encouraged starting  
 157 on Mar 8<sup>6</sup>, but mass gatherings still occurred on Mar 8, including a march of 120,000 people for the  
 158 [International Women's Day](#), and a football match between [Real Betis](#) and [Real Madrid](#) (2:1) with a  
 159 crowd of 50,965 in Seville. A national lockdown was only announced on Mar 14<sup>6</sup>. Nevertheless, we  
 160 estimate the effective start of NPI  $\hat{\tau}$  on Mar 8 or 9 ( $\pm 1.08$  95%CI), rather than Mar 14 (Figure 3).

161 Similarly, in France we estimate the effective start of NPIs  $\hat{\tau}$  on Mar 8 or Mar 9 ( $\pm 6.27$  days 95% CI,  
 162 Figure 3). Although the credible interval is wider compared to Spain, spanning from Mar 2 to Mar 15,  
 163 the official lockdown start at Mar 17 is later still, and even the earliest NPI, banning of public events,  
 164 only started on Mar 13<sup>6</sup>.

165 Interestingly, the effective start of NPIs  $\hat{\tau}$  in both France and Spain is estimated at Mar 8, although  
 166 the official NPI dates differ significantly: the first NPI in France is only one day before the last NPI in  
 167 Spain. The number of daily cases was similar in both countries until Mar 8, but diverged by Mar 13,  
 168 reaching significantly higher numbers in Spain (Figure S3). This may suggest that correlation exist  
 169 between effective start of NPIs due to global or international events.

170 **The exception that proves the rule.** We find one case in which the official and effective dates match:  
 171 Switzerland ordered a national lockdown on Mar 20, after banning public events and closing schools  
 172 on Mar 13 and 14<sup>6</sup>. Indeed, the posterior median  $\hat{\tau}$  is Mar 20 ( $\pm 8.46$  days 95% CI), and the posterior  
 173 distribution shows two density peaks: a smaller one between Mar 10 and Mar 14, and a bigger one  
 174 between Mar 17 and Mar 22 (??). It's also worth mentioning that Switzerland was the first to mandate  
 175 self isolation of confirmed cases<sup>6</sup>.

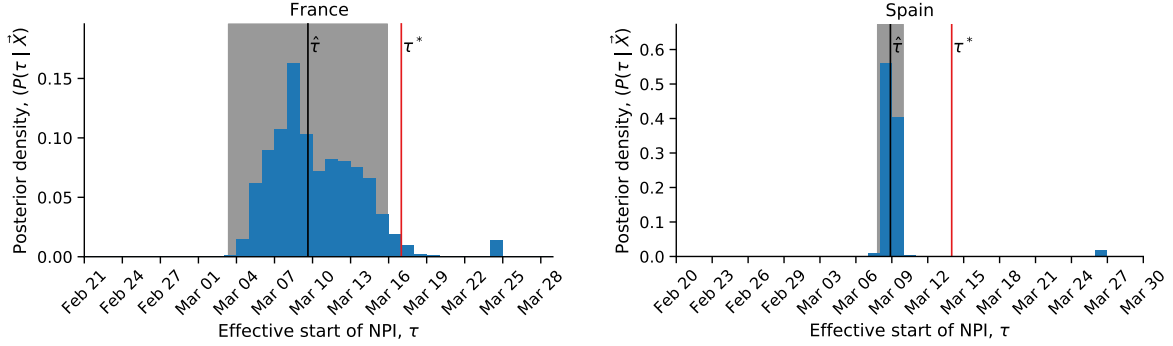


**Figure 3: Early effect of non-pharmaceutical interventions in France and Spain.** Posterior distribution of  $\tau$ , the effective start date of NPI, is shown as a histogram of MCMC samples. Red line shows the official last NPI date  $\tau^*$ . Black line shows the estimated  $\hat{\tau}$ . Shaded area shows a 95% credible interval (area in which  $P(|\tau - \hat{\tau}| \mid \mathbf{X}) = 0.95$ ).

176 **Effect of late and early effect of NPIs on real-time assessment.** The success of non-pharmaceutical  
 177 interventions is assessed by health officials using various metrics, such as the decline in the growth  
 178 rate of daily cases. These assessments are made a specific number of days after the intervention began,  
 179 to accommodate for the expected serial interval<sup>3</sup> (i.e. time between successive cases in a chain of  
 180 transmission), which is estimated at about 4-7 days<sup>8</sup>.

181 However, a significant difference between the beginning of the intervention and the effective change in  
 182 transmission rates can invalidate assessments that assume a serial interval of 4-7 days and neglect the  
 183 late or early population response to the NPI. This is illustrated in Figure 4 using data and parameters  
 184 from Italy. Here, a lockdown is officially ordered on Mar 10 ( $\tau^*$ ), but its late effect on the transmission  
 185 dynamics starts on Mar 16 ( $\hat{\tau}$ ). If health officials assume the dynamics to immediately change at  $\tau^*$ ,  
 186 they will expect the number of cases be within the red lines (posterior predictions assuming  $\tau = \tau^*$ ).  
 187 This leads to a significant underestimation, which might be interpreted by officials as ineffectiveness  
 188 of NPIs, leading to further escalations. However, the number of cases will actually follow the blue  
 189 lines (posterior predictions using  $\tau = \hat{\tau}$ ), which corresponds well to the real data.

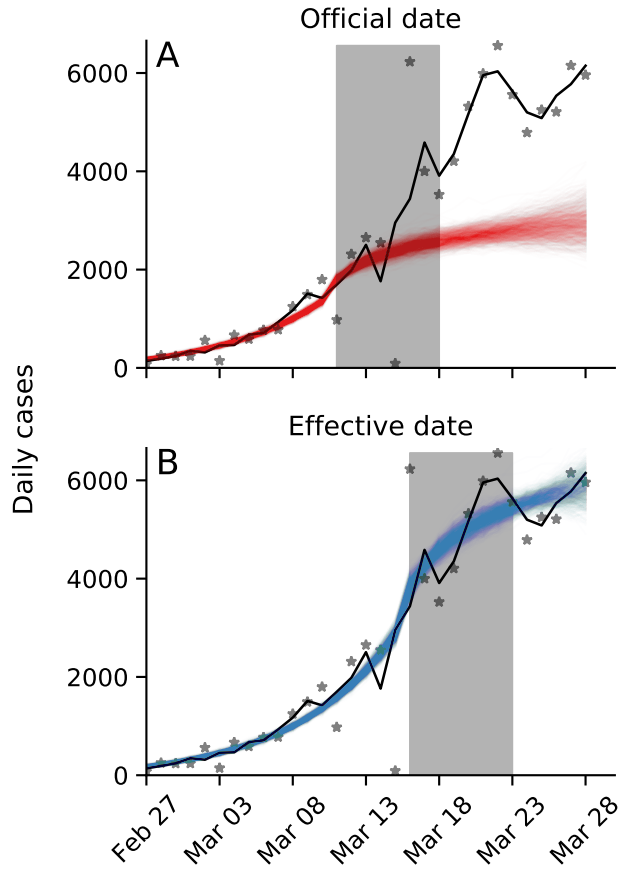


**Figure 4: Late effective start of NPIs leads to under-estimation of daily confirmed cases.** Real number of daily cases in Italy in black (markers: data, line: time moving average). Model posterior predictions are shown as colored lines (1,000 draws from the posterior distribution). Shaded box illustrates a serial interval of seven days. **(A)** Using the official date  $\tau^*$  for the start of the NPI, the model under-estimates the number of cases seven days after the start of the NPI. **(B)** Using the effective date  $\hat{\tau}$  for the start of the NPI, the model correctly estimates the number of cases seven days after the start of the NPI. Here, model parameters are estimates for Italy (Table 2).

## 190 Discussion

191 We have estimated the effective start date of NPIs in several geographical regions using an SEIR  
 192 epidemiological model and an MCMC parameter estimation framework. We find examples of both  
 193 late and early effect of NPIs (Figure 1).

194 For example, in Italy and Wuhan, China, the effective start of the lockdowns seems to have occurred  
 195 more than five days after the official date (Figure 2). This difference might be explained by low  
 196 compliance: In Italy, for example, the government intention to lockdown Northern provinces leaked  
 197 to the public, resulting in people leaving those provinces<sup>8</sup>. Late effect of NPIs might also be due to  
 198 the time required by both the government and the citizens to organize for a lockdown, and for the new  
 199 guidelines to diffuse in the population.

200 In contrast, in most investigated countries (e.g., Spain and France), we infer reduced transmission  
 201 rates even before official lockdowns were implemented (Figure 3). An early effective date might be  
 202 due to adoption of social distancing and similar behavioral adaptations in parts of the population,  
 203 maybe in response to increased risk perception due to domestic or international COVID-19-related  
 204 reports. This finding may also suggest that severe NPIs, such as lockdowns, were unnecessary, and  
 205 that less extreme measures adopted by the population could have been sufficient for epidemic control.

206 These less extreme measures may have been implemented due to government recommendations, media  
207 coverage, and social networks, rather than official NPIs. Indeed, the evidence supports a change in  
208 transmission dynamics (i.e. a model with free  $\tau$ ) even for Sweden (Figure S2a), in which a lockdown  
209 was not implemented\*, suggesting that lockdowns may not be necessary if other NPIs are adopted  
210 early enough during the outbreak<sup>3</sup>.

211 Attempts to assess the effect of NPIs<sup>3,6</sup> generally assume a seven days delay between the implementation  
212 of the intervention and the observable change in dynamics, due to the characteristic serial interval of  
213 COVID-19<sup>8</sup>. However, the late and early effects we have estimated can confuse these assessments and  
214 lead to wrong conclusions about the effects of NPIs (Figure 4).

215 We have found that the evidence supports a model in which the parameters change at a specific  
216 time point  $\tau$  over a model without such a change-point. It may be interesting to investigate if the  
217 evidence favors a model with two change-points, rather than one. Two such change-points could reflect  
218 escalating NPIs (e.g. school closures followed by lockdowns), or a mix of NPIs and other events, such  
219 as weather, or domestic and international events that affect risk perception.

220 As several countries (e.g. Austria, Israel) begin to relieve lockdowns and ease restrictions, we expect  
221 similar delays and advances to occur: in some countries people will begin to behave as if restrictions  
222 were eased even before the official date, and in some countries people will continue to self-restrict  
223 even after restrictions are officially removed.

224 **Conclusions.** We have estimated the effective start date of NPIs and found that they often differ from  
225 the official dates. Our results highlight the complex interaction between personal, regional, and global  
226 determinants of behavioral response to infectious disease. Therefore, we emphasize the need to further  
227 study variability in compliance and behavior over both time and space. This can be accomplished  
228 both by surveying differences in compliance within and between populations<sup>2</sup>, and by incorporating  
229 specific behavioral models into epidemiological models<sup>1,5,16</sup>.

## 230 Acknowledgements

231 We thank Lilach Hadany and Oren Kolodny for discussions and comments. This work was supported in part by  
232 the Israel Science Foundation 552/19 and 1399/17.

---

\*Sweden banned public events on Mar 12, encouraged social distancing on Mar 16, and closed schools on Mar 18<sup>6</sup>.

- [1] Arthur, R. F., Jones, J. H., Bonds, M. H. and Feldman, M. W. 2020, ‘Complex dynamics induced by delayed adaptive behavior during outbreaks’, *bioRxiv* pp. 1–23.
- [2] Atchison, C. J., Bowman, L., Vrinten, C., Redd, R., Pristera, P., Eaton, J. W. and Ward, H. 2020, ‘Perceptions and behavioural responses of the general public during the COVID-19 pandemic: A cross-sectional survey of UK Adults’, *medRxiv* p. 2020.04.01.20050039.
- [3] Banholzer, N., Weenen, E. V., Kratzwald, B. and Seeliger, A. 2020, ‘The estimated impact of non-pharmaceutical interventions on documented cases of COVID-19 : A cross-country analysis’, *medRxiv*.
- [4] Dunn, A. G., Leask, J., Zhou, X., Mandl, K. D. and Coiera, E. 2015, ‘Associations between exposure to and expression of negative opinions about human papillomavirus vaccines on social media: An observational study’, *J. Med. Internet Res.* **17**(6), e144.
- [5] Fenichel, E. P., Castillo-Chavez, C., Cediac, M. G., Chowell, G., Gonzalez Parrae, P. A., Hickling, G. J., Holloway, G., Horan, R., Morin, B., Perrings, C., Springborn, M., Velazquez, L. and Villalobos, C. 2011, ‘Adaptive human behavior in epidemiological models’, *Proc. Natl. Acad. Sci. U. S. A.* **108**(15), 6306–6311.
- [6] Flaxman, S., Mishra, S., Gandy, A., Unwin, J. T., Coupland, H., Mellan, T. A., Zhu, H., Berah, T., Eaton, J. W., Guzman, P. N. P., Schmit, N., Cilloni, L., Ainslie, K. E. C., Baguelin, M., Blake, I., Boonyasiri, A., Boyd, O., Cattarino, L., Ciavarella, C., Cooper, L., Cucunubá, Z., Cuomo-Dannenburg, G., Dighe, A., Djaafara, B., Dorigatti, I., Van Elsland, S., Fitzjohn, R., Fu, H., Gaythorpe, K., Geidelberg, L., Grassly, N., Green, W., Hallett, T., Hamlet, A., Hinsley, W., Jeffrey, B., Jorgensen, D., Knock, E., Laydon, D., Nedjati-Gilani, G., Nouvellet, P., Parag, K., Siveroni, I., Thompson, H., Verity, R., Volz, E., Gt Walker, P., Walters, C., Wang, H., Wang, Y., Watson, O., Xi, X., Winskill, P., Whittaker, C., Ghani, A., Donnelly, C. A., Riley, S., Okell, L. C., Vollmer, M. A. C., Ferguson, N. M. and Bhatt, S. 2020, ‘Estimating the number of infections and the impact of non-pharmaceutical interventions on COVID-19 in 11 European countries’, *Imp. Coll. London* (March), 1–35.
- [7] Foreman-Mackey, D., Hogg, D. W., Lang, D. and Goodman, J. 2013, ‘emcee : The MCMC Hammer’, *Publ. Astron. Soc. Pacific* **125**(925), 306–312.
- [8] Gatto, M., Bertuzzo, E., Mari, L., Miccoli, S., Carraro, L., Casagrandi, R. and Rinaldo, A. 2020, ‘Spread and dynamics of the COVID-19 epidemic in Italy: Effects of emergency containment measures’, *Proc. Natl. Acad. Sci.* p. 202004978.
- [9] Gelman, A., Carlin, J. B., Stern, H. S., Dunson, D. B., Vehtari, A. and Rubin, D. B. 2013, *Bayesian Data Analysis, Third Edition*, Chapman & Hall/CRC Texts in Statistical Science, Taylor & Francis.
- [10] Goodman, J. and Weare, J. 2010, ‘Ensemble Samplers With Affine Invariance’, *Commun. Appl. Math. Comput. Sci.* **5**(1), 65–80.
- [11] Kaufman, M. R., Cornish, F., Zimmerman, R. S. and Johnson, B. T. 2014, ‘Health behavior change models for HIV prevention and AIDS care: Practical recommendations for a multi-level approach’, *J. Acquir. Immune Defic. Syndr.* **66**(SUPPL.3), 250–258.
- [12] Li, R., Pei, S., Chen, B., Song, Y., Zhang, T., Yang, W. and Shaman, J. 2020, ‘Substantial undocumented infection facilitates the rapid dissemination of novel coronavirus (SARS-CoV2)’, *Science* (80-. ). p. eabb3221.
- [13] Pei, S. and Shaman, J. 2020, ‘Initial Simulation of SARS-CoV2 Spread and Intervention Effects in the Continental US’, *medRxiv* p. 2020.03.21.20040303.
- [14] Smith, L. E., Mottershaw, A. L., Egan, M., Waller, J., Marteau, T. M. and Rubin, G. J. 2020, ‘The impact of believing you have had COVID-19 on behaviour : Cross-sectional survey’, *medRxiv* pp. 1–20.
- [15] Spiegelhalter, D. J., Best, N. G., Carlin, B. P. and Van Der Linde, A. 2002, ‘Bayesian measures of model complexity and fit’, *J. R. Stat. Soc. Ser. B Stat. Methodol.* **64**(4), 583–616.
- [16] Walters, C. E. and Kendal, J. R. 2013, ‘An SIS model for cultural trait transmission with conformity bias’, *Theor. Popul. Biol.* **90**, 56–63.
- [17] Wiyeh, A. B., Cooper, S., Nnaji, C. A. and Wiysonge, C. S. 2018, ‘Vaccine hesitancy

- âĂŹoutbreaks’: using epidemiological modeling of the spread of ideas to understand the effects of vaccine related events on vaccine hesitancy’, *Expert Rev. Vaccines* **17**(12), 1063–1070.
- [18] Zipfel, C. M. and Bansal, S. 2020, ‘Assessing the interactions between COVID-19 and influenza in the United States’, *medRxiv* (February), 1–13.

234 **Supplementary Material**

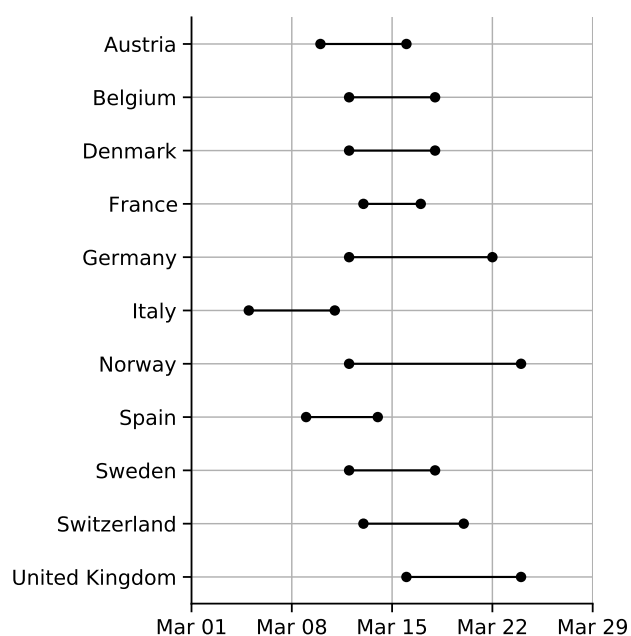
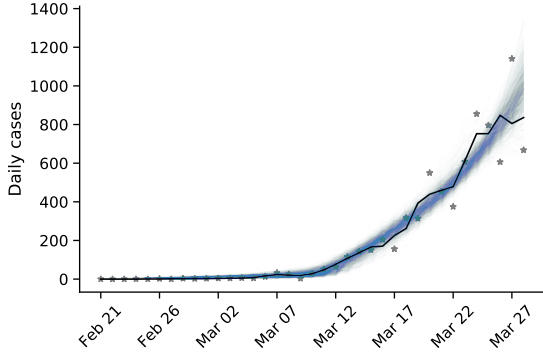
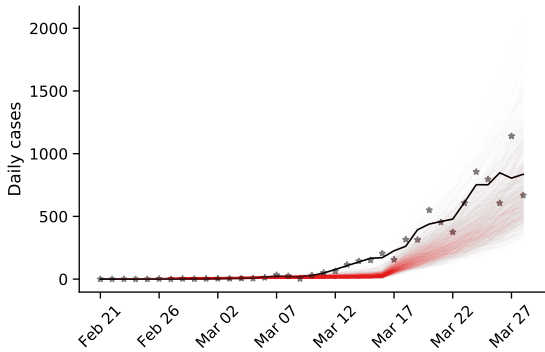


**Figure S1: Official start of non-pharmaceutical interventions.** See Table S1 for more details. Wuhan, China is not shown.

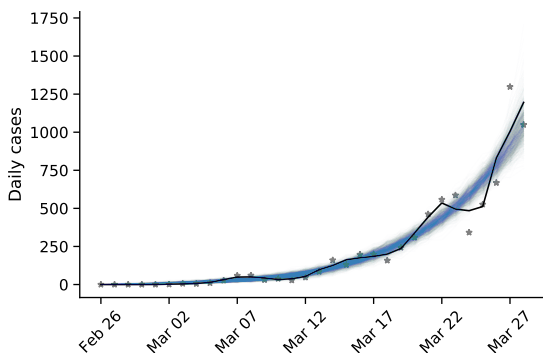
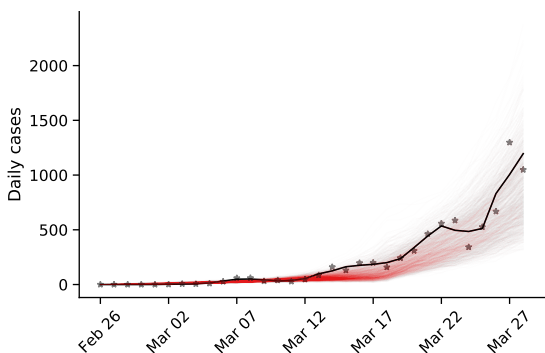
Country	Fixed	Free	No
Austria	26.68	29.80	39.73
Belgium	29.38	30.62	28.81
Denmark	38.56	37.29	49.63
France	50.04	50.59	72.17
Germany	214.99	174.24	310.69
Italy	301.52	233.13	609.26
Norway	34.21	36.07	37.54
Spain	59.90	92.55	141.60
Sweden	25.93	25.86	28.36
Switzerland	74.85	73.07	99.74
United Kingdom	38.10	37.49	35.77
Wuhan China	94.12	74.10	107.34

**Table S1: WAIC values for the different models.** WAIC (widely applicable information criterion)<sup>9</sup> values for models with: *No*: no  $\tau$  at all; *Fixed*:  $\tau$  fixed at the official last NPI date  $\tau^*$ ; and *Free*: free  $\tau$ . WAIC values are scaled as a deviance measure: lower values imply higher predictive accuracy.

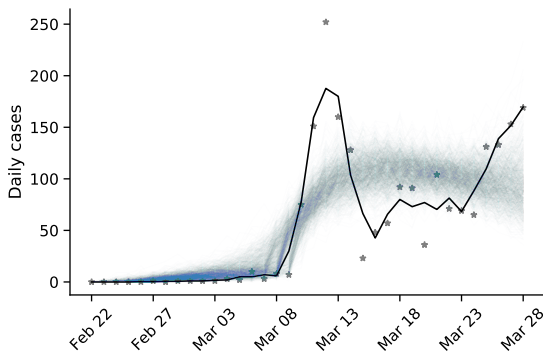
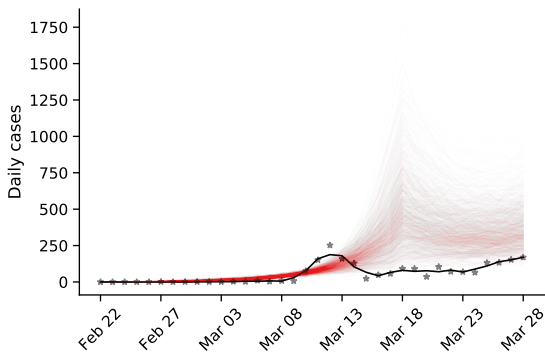
Austria



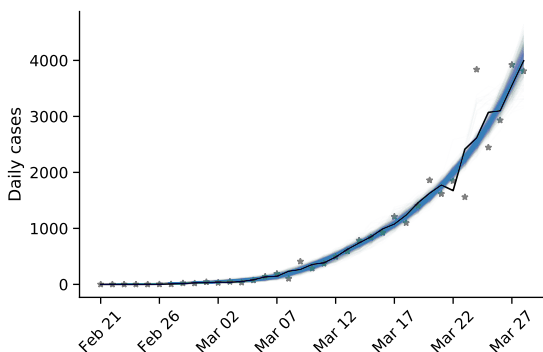
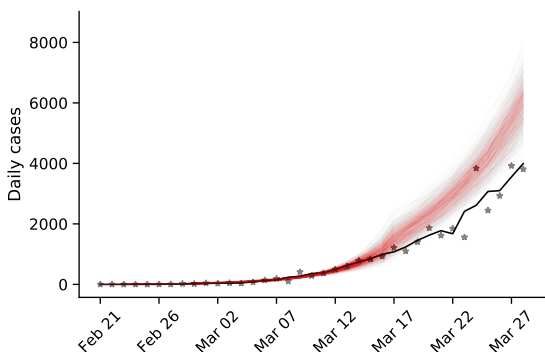
Belgium



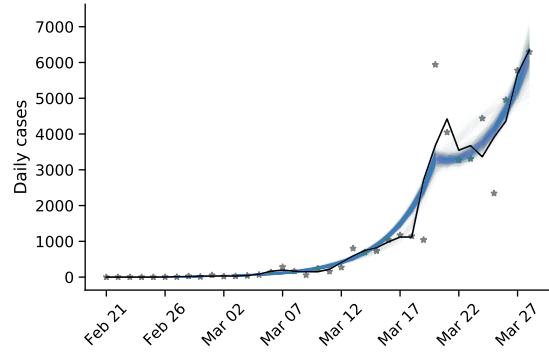
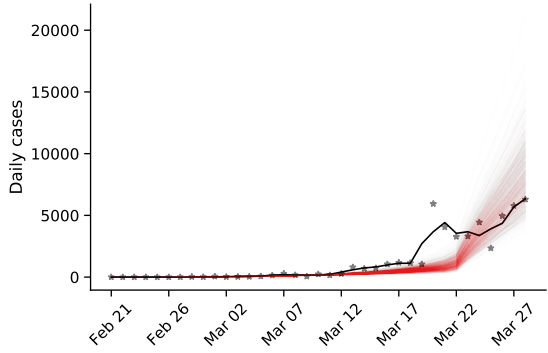
Denmark



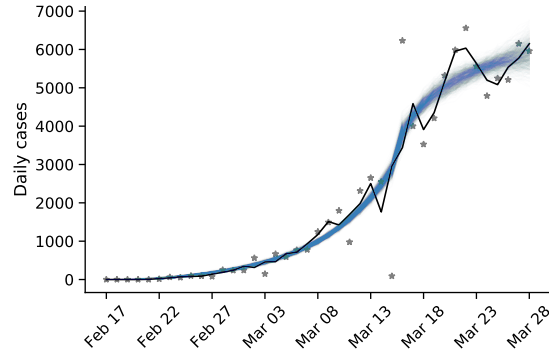
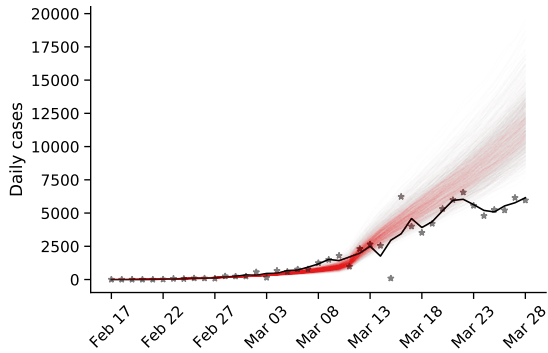
France



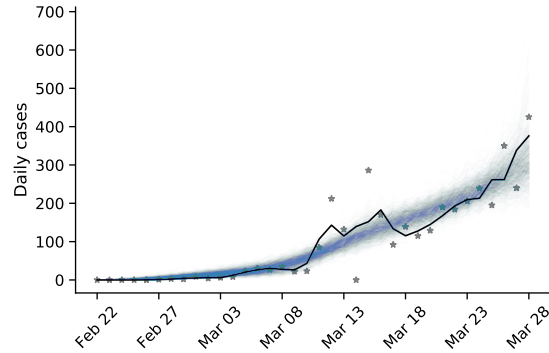
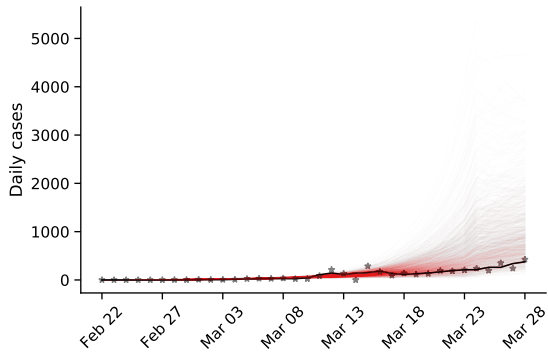
Germany



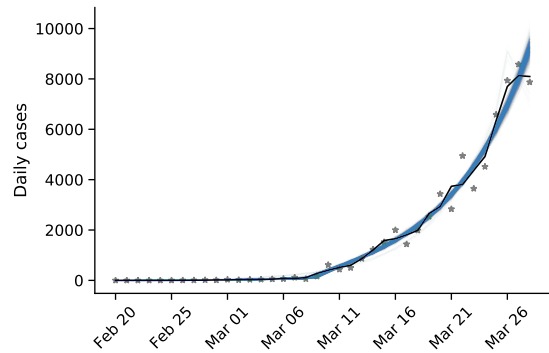
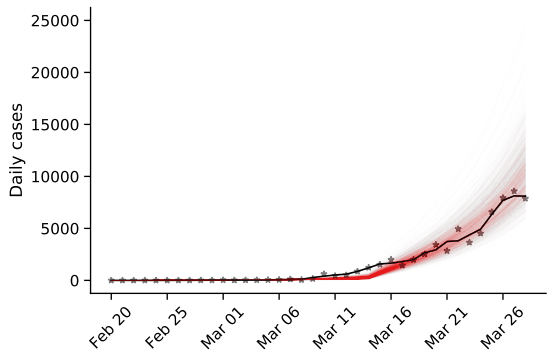
Italy



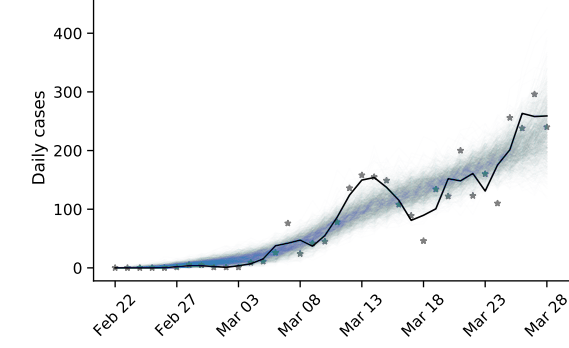
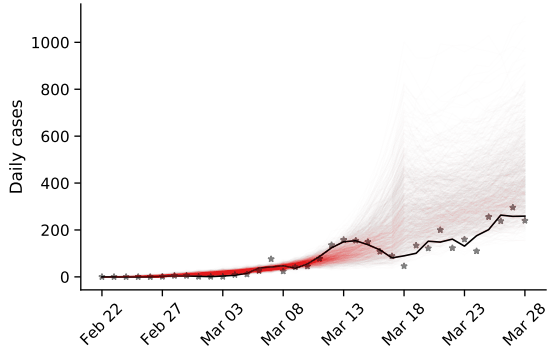
Norway



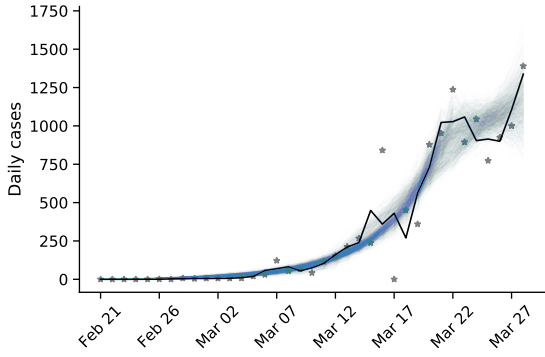
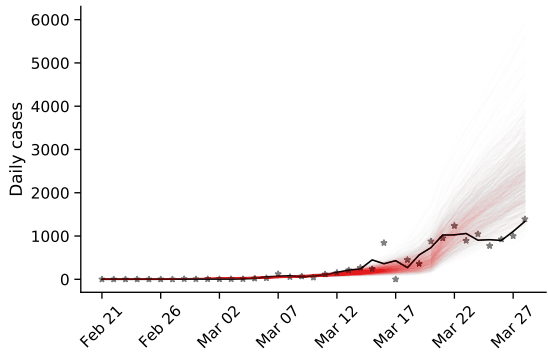
Spain



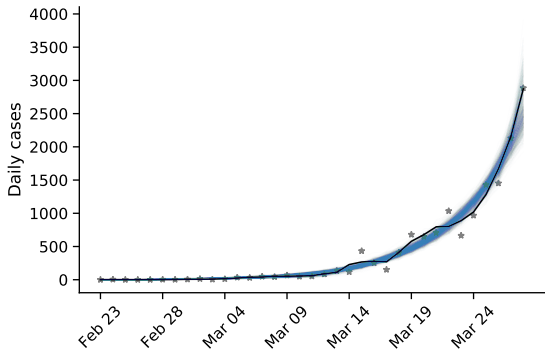
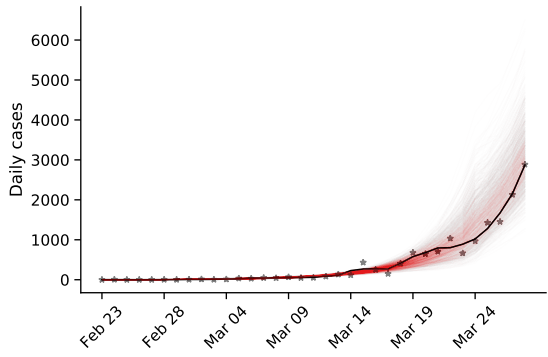
## Sweden



## Switzerland



## United Kingdom



## Wuhan, China

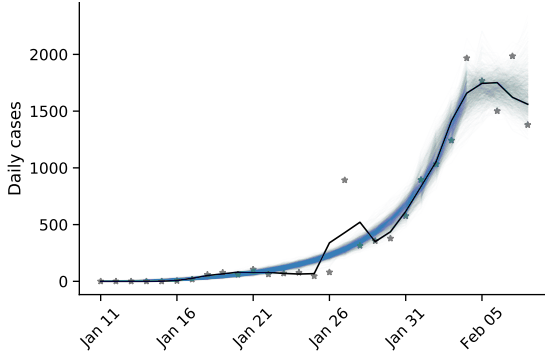
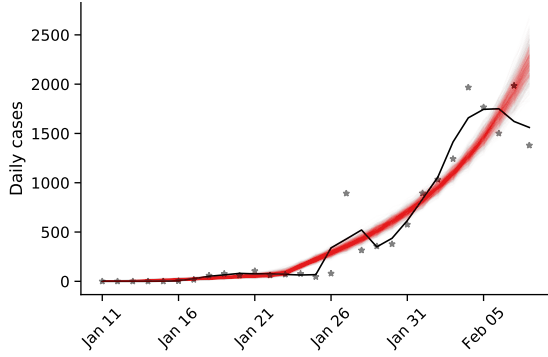


**Figure S2. Posterior prediction check plots** Markers represent data ( $\mathbf{X}$ ). Black line represent a smoothing of the data points using a Savitzky-Golay filter. Color lines represent posterior predictions from a model with fixed  $\tau$ , in red, and free  $\tau$ , in blue. These predictions are made by drawing 1,000 samples from the parameter posterior distribution and then generating a daily case count using the SEIR model in Eq. (1). Note the differences in the y-axis scale.

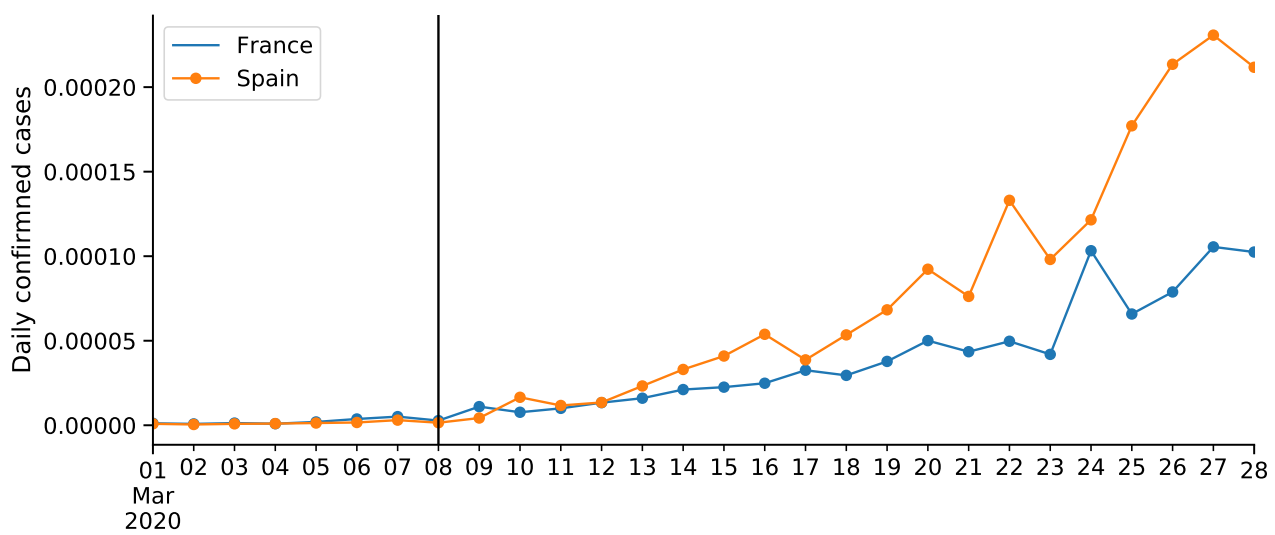


**Figure S3: COVID-19 confirmed cases in France and Spain.** Number of cases proportional to population size (as of 2018). Vertical line shows Mar 8, the effective start of NPIs  $\hat{\tau}$  in both countries.